Electronic Supporting Information

for

Evaluating Prussian Blue Analogues $M^{II}_3[M^{III}(CN)_6]_2$ (M^{II} = Co, Cu, Fe, Mn, Ni; M^{III} = Co, Fe) as Activators for Peroxymonosulfate in Water

Kun-Yi Andrew Lin [a,*], *Bo-Jau Chen*[a], *and Chih-Kuang Chen* [b,*]

[a]Department of Environmental Engineering, National Chung Hsing University, 250 Kuo-Kuang Rd., Taichung, Taiwan

[b]Department of Fiber and Composite Materials, Feng-Chia University, 100 Wenhwa Rd., Taichung, Taiwan

*Corresponding Author. Tel: +886-4-22854709, E-mail address: linky@nchu.edu.tw (Kun-Yi Andrew Lin); chihkuan@mail.fcu.edu.tw (Chih-Kuang Chen)

Section S1. Activation of peroxymonosulfate by $Co[Co(CN)_6]_2$ (Co-Co)

S1.1 Effects of PBA loading and PMS dosage

On the other hand, we selected $Co_3[Co(CN)_6]_2$ (Co-Co) to further investigate PMS activation by $[Co(CN)_6]_2$-based PBAs under various conditions. The effect of PBA loading was first examined (Fig. S9(a)). The higher loading of Co-Co also allowed a higher and faster RhB decolorization. While 10 mg L^{-1} of Co-Co was less effective than 50 and 100 mg L^{-1} of Co-Co for activating PMS, 10 mg L^{-1} of Co-Co had still exhibited much more decolorization extent than 50 mg L^{-1} of Co_3O_4, demonstrating high activating capability of Co-Co for PMS.

Fig. S9(b) reveals the effect of PMS on RhB decolorization. When PMS dosage increased, RhB in water was completely decolorized within shorter times. This suggests that a sufficient dosage of PMS is required in order to generate sufficient sulfate radicals for decolorization as Co-Co acted as a catalyst instead of a source of sulfate radicals.

S1.2 Effects of temperature

RhB decolorization using PMS activated by Co-Co at different temperatures is shown in Fig. S10. The corresponding k_1 values at different temperatures are summarized in Table 2. Similar to Co-Fe, RhB decolorization kinetics became noticeably faster at higher temperatures. A plot of ln k_1 versus $1/T$ is shown as the inset of Fig. S10, in which data points are also well-fit by linear regression, suggesting that the rate of PMS activation by Co-Co can be associated with temperature via the Arrhenius equation. The corresponding E_a is determined as 44.8 kJ mol^{-1}.

S1.3 Effects of pH and salt

RhB decolorization using PMS activated by Co-Co under acidic, neutral and alkaline conditions is displayed in Fig. S11(a). As discussed in the earlier section, the

electrostatic repulsion between RhB and Co-Co might increase under acidic conditions, limiting contact between RhB and sulfate radicals present on Co-Co surface. Under alkaline conditions, PMS activation might be significantly hindered and could not generate sulfate radicals for decolorization, leading to ineffective decolorization at relative high pH values. The pH variation of PMS activation by Co-Co was also measured and shown in Fig. S7(b). Similar to the pH variation of PMS activation by Co-Fe, pH of RhB solution was not considerably changed and pH also approached an equilibrium pH of ~5, indicating that PMS activation by Co-Co can also proceed under a relatively stable condition.

Fig. S11(b) reveals RhB decolorization using PMS activated by Co-Co in the presence of NaCl. Even though the concentration of NaCl was 1000 and 2000 mg L^{-1}, Co-Co remained quite effective to activate PMS even with concentrated NaCl.

S1.4 Effects of inhibitors and decolorization mechanism

Fig. S12(a) shows that RhB decolorization was also completely inhibited in the presence of ascorbic acid, demonstrating the critical role of radicals for decolorizing RhB in water. When TBA was then evaluated, RhB decolorization extent was considerably diminished as k_1 reduced from 0.56 to 0.12 min^{-1} and C_t/C_0 reached 0.3, suggesting that RhB decolorization was associated with $OH^{\bullet}$. On the other hand, RhB decolorization was significantly inhibited in the presence of methanol as k_1 decreased from 0.56 to 0.01 min^{-1} and C_t/C_0 only reached 0.9. This suggests that PMS activation by Co-Co is primarily attributed to $SO_4^{\bullet-}$ and $OH^{\bullet}$ to a lesser extent.

S1.5 Recyclability of $Co_3[Co(CN)_6]_2$ for activating PMS

Fig. S12(b) demonstrates a multi-cycle test of using Co-Co for activating PMS to decolorize RhB. As decolorization extent remained comparable over 6 cycles, reused Co-Co was considered as effective as pristine Co-Co for activating PMS. The

crystalline structure of Co-Co also remained intact over multiple cycles (Fig. S8 (b)). This indicates that Co-Co can be also an efficient, recyclable and durable catalyst for PMS activation.

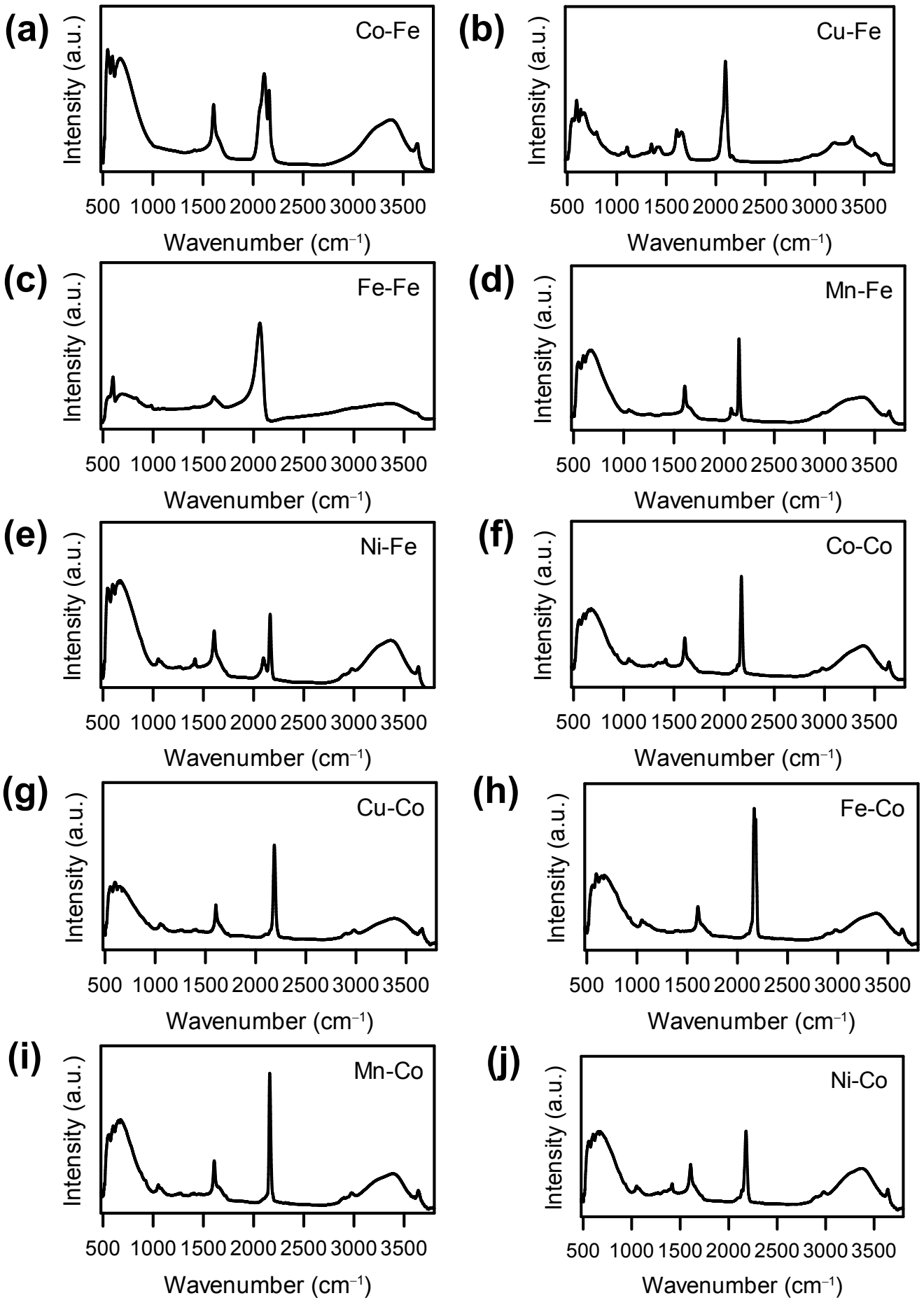

Fig. S1. IR spectra of (a) Co-Fe, (b) Cu-Fe, (c) Fe-Fe, (d) Mn-Fe, (e) Ni-Fe, (f) Co-Co, (g) Cu-Co, (h) Fe-Co, (i) Mn-Co and (j) Ni-Co.

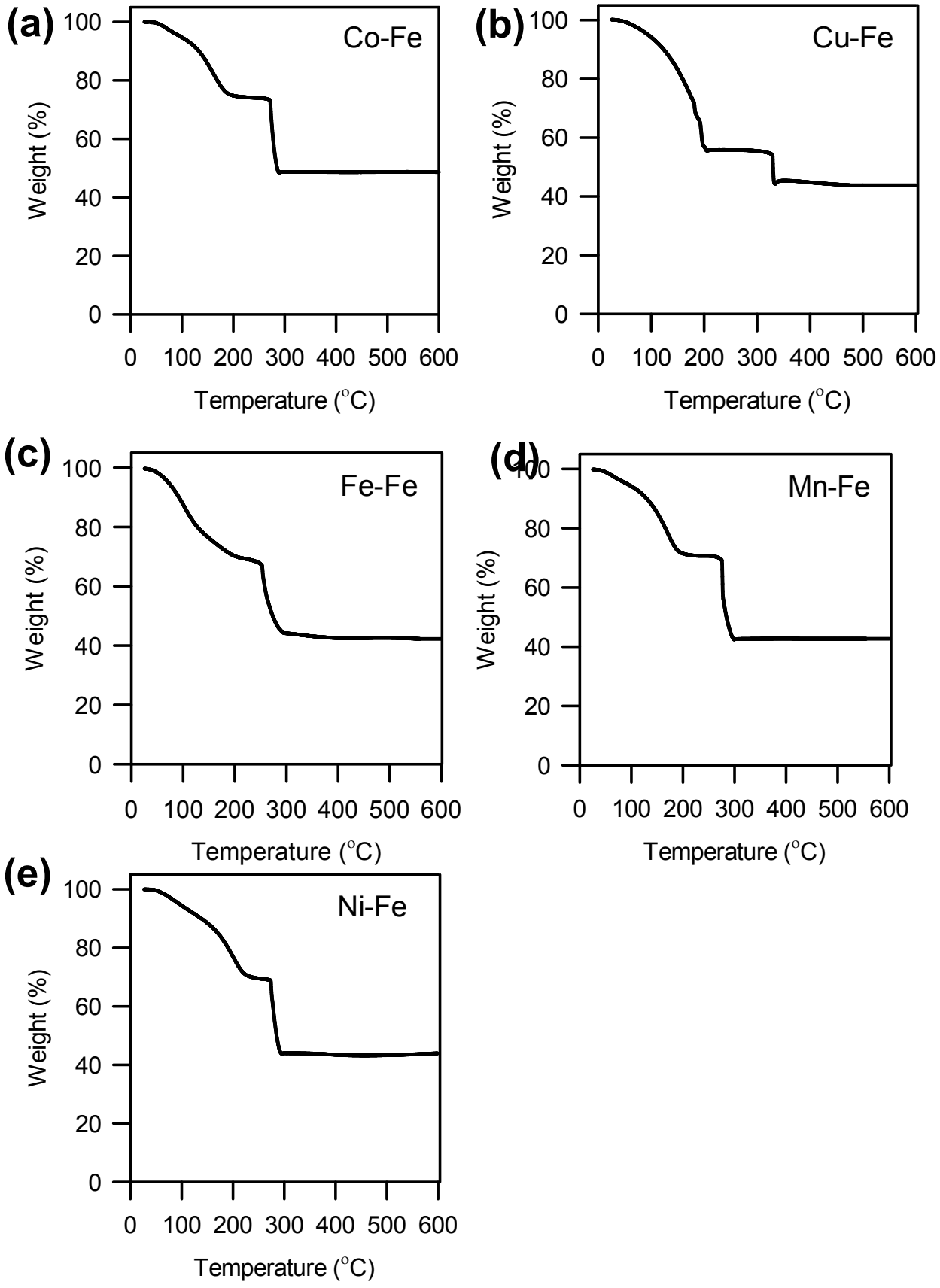

Fig. S2. Thermogravimetric analyses of $M^{II}_3[Fe(CN)_6]_2$: (a) $Co_3[Fe(CN)_6]_2$, (b) $Cu_3[Fe(CN)_6]_2$, (c) $Fe_3[Fe(CN)_6]_2$, (d) $Mn_3[Fe(CN)_6]_2$, (e) $Ni_3[Fe(CN)_6]_2$.

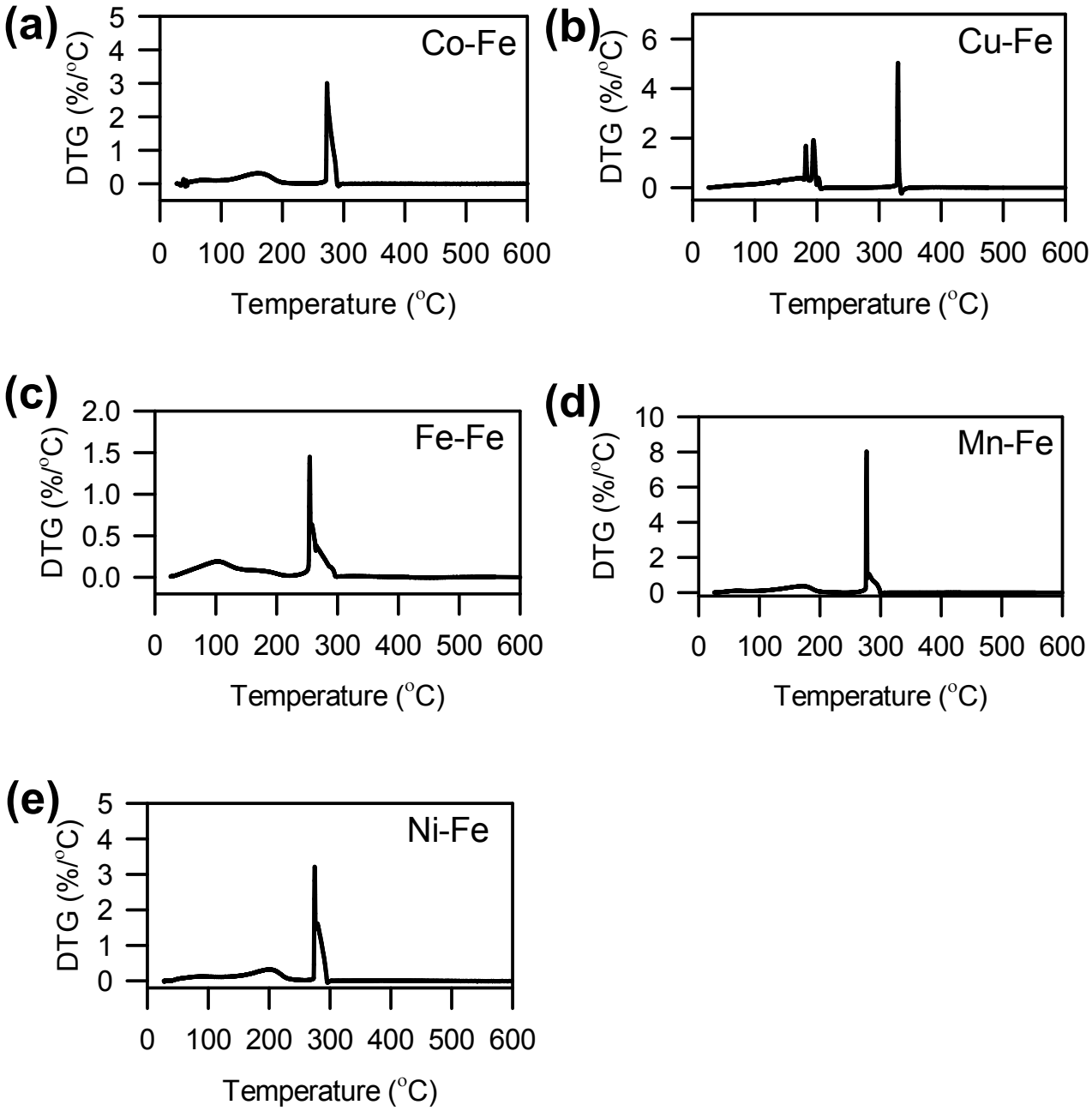

Fig. S3. Derivative thermogravimetric analyses of $M^{II}_3[Fe(CN)_6]_2$: (a) $Co_3[Fe(CN)_6]_2$, (b) $Cu_3[Fe(CN)_6]_2$, (c) $Fe_3[Fe(CN)_6]_2$, (d) $Mn_3[Fe(CN)_6]_2$, (e) $Ni_3[Fe(CN)_6]_2$.

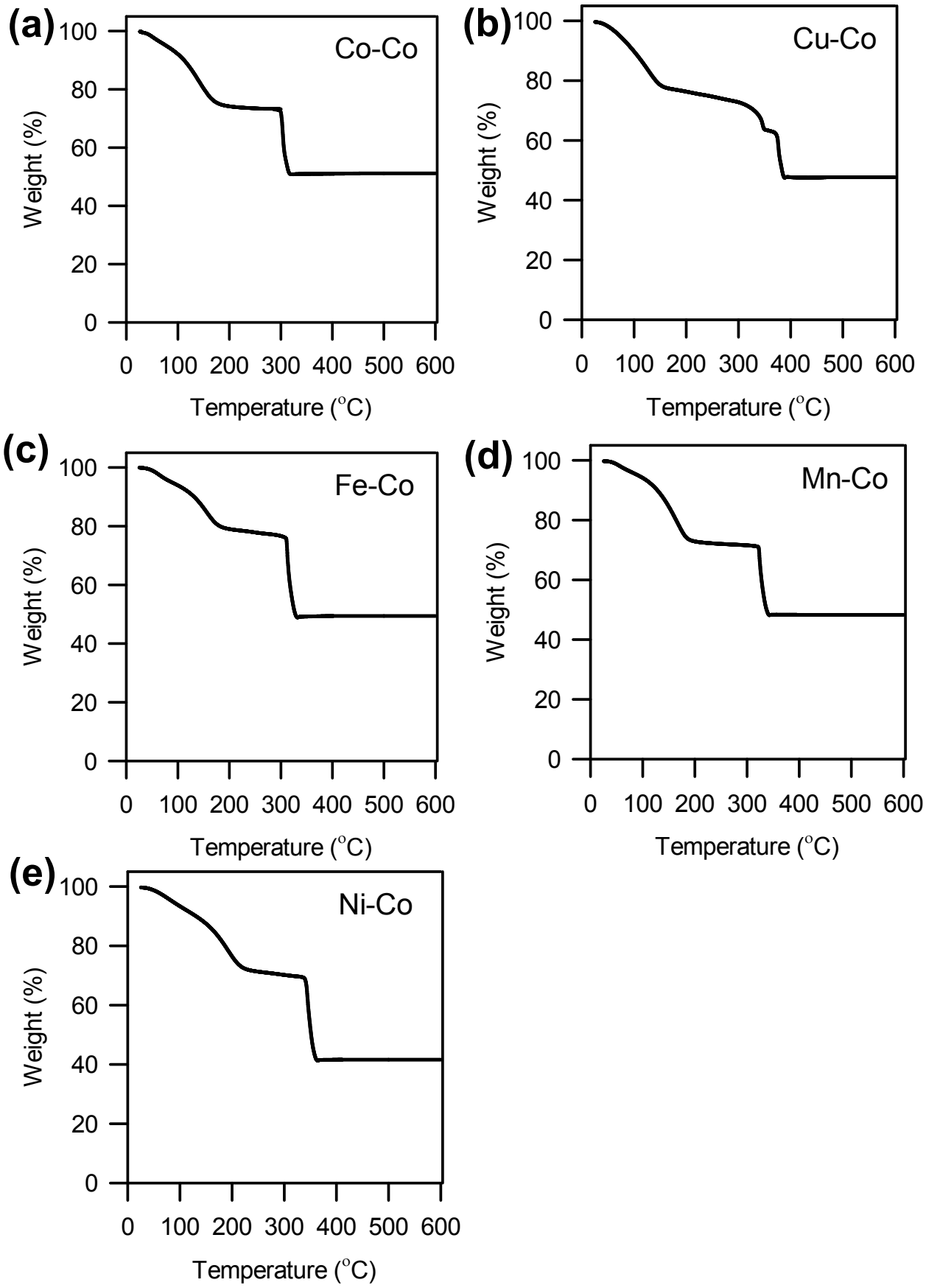

Fig. S4. Thermogravimetric analyses of $M^{II}_3[Co(CN)_6]_2$: (a) $Co_3[Co(CN)_6]_2$, (b) $Cu_3[Co(CN)_6]_2$, (c) $Fe_3[Co(CN)_6]_2$, (d) $Mn_3[Co(CN)_6]_2$, (e) $Ni_3[Co(CN)_6]_2$.

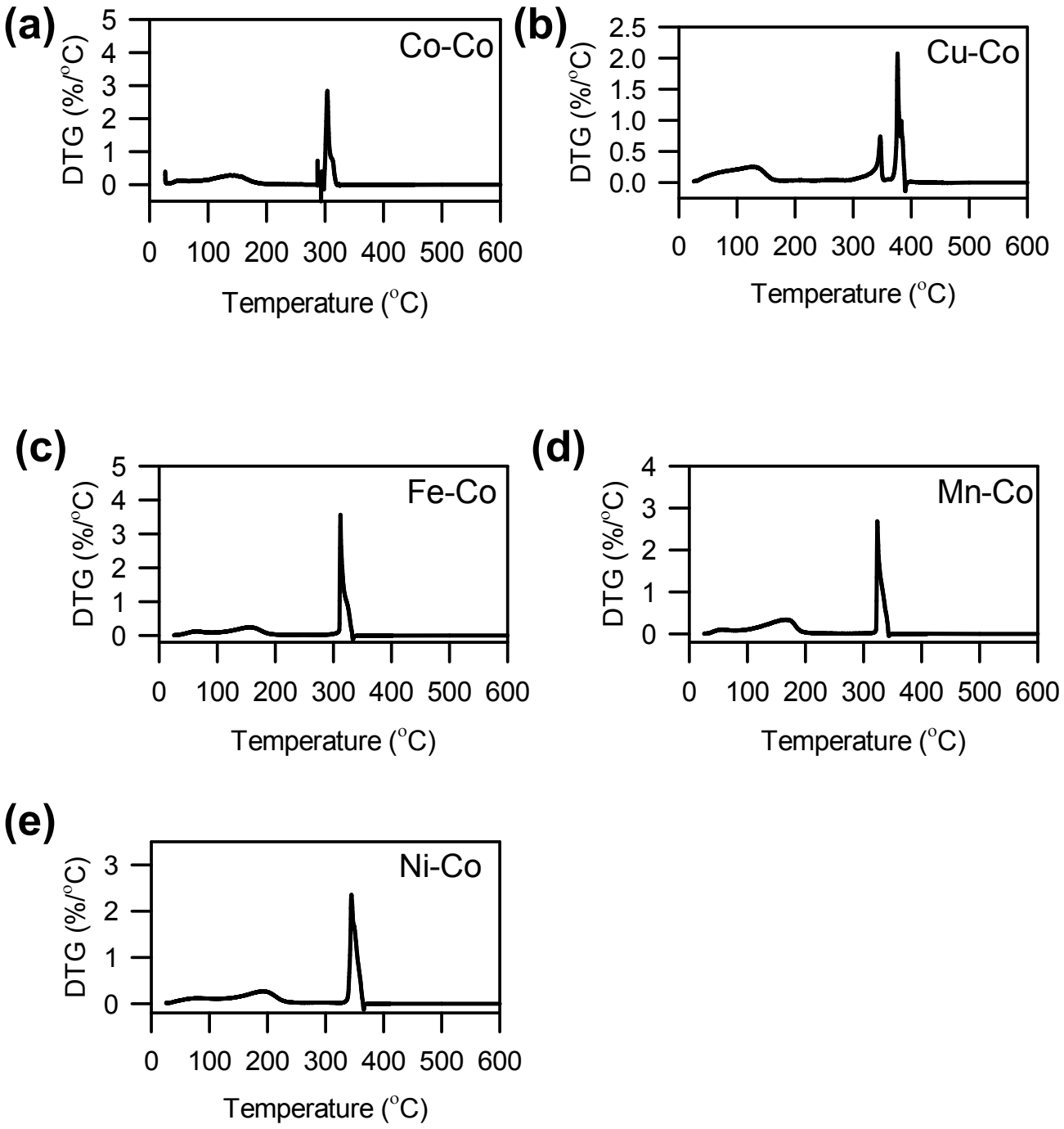

Fig. S5. Derivative thermogravimetric analyses of $M^{II}_3[Co(CN)_6]_2$: (a) $Co_3[Co(CN)_6]_2$, (b) $Cu_3[Co(CN)_6]_2$, (c) $Fe_3[Co(CN)_6]_2$, (d) $Mn_3[Co(CN)_6]_2$, (e) $Ni_3[Co(CN)_6]_2$.

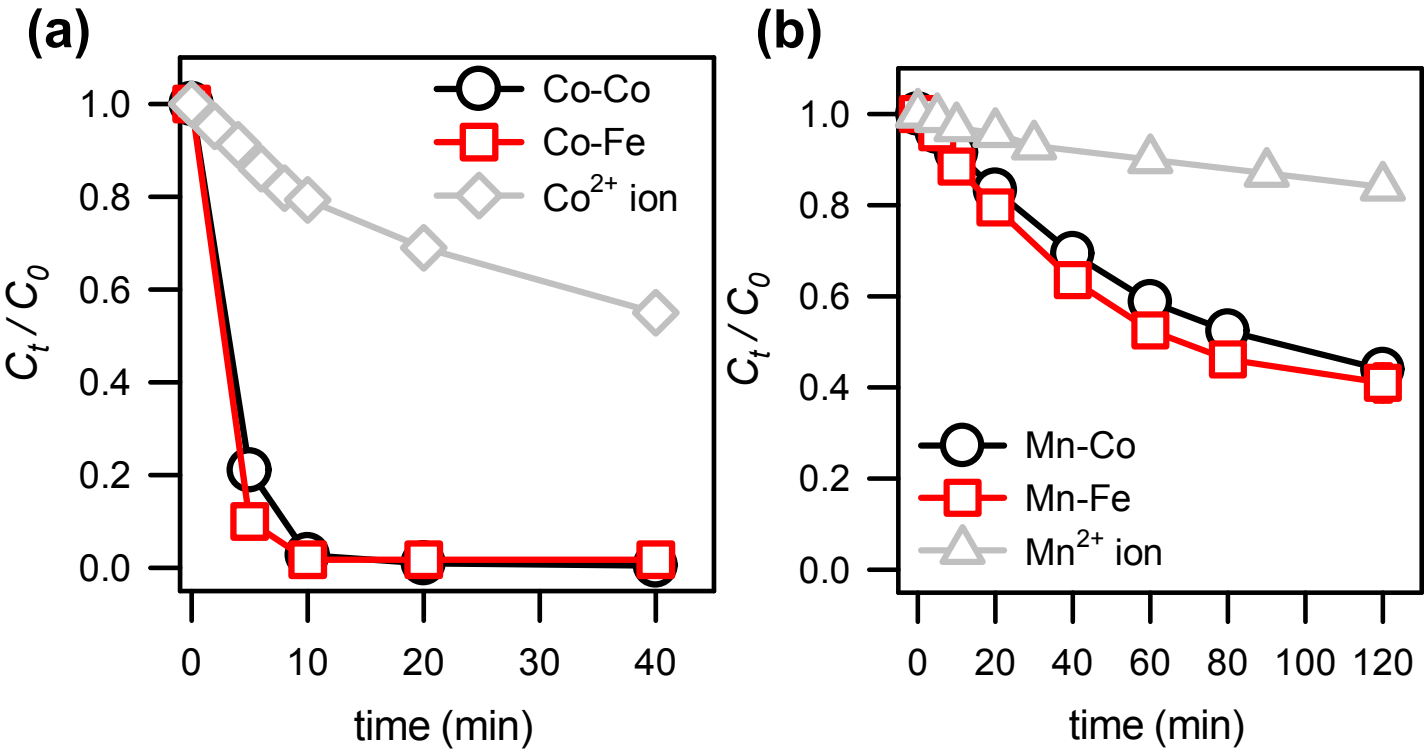

Fig. S6. A comparison of RhB decolorization using PMS activated by PBAs (*i.e.*, (a) Co-Fe and Co-Co; (b) Mn-Fe and Mn-Co) and homogeneous Co^{2+}/Mn^{2+} ions (Co^{2+} = 0.2 mg L^{-1} and Mn^{2+} = 0.4 mg L^{-1}). (PBA = 50 mg L^{-1}, PMS = 50 mg L^{-1}, T = 30 °C)

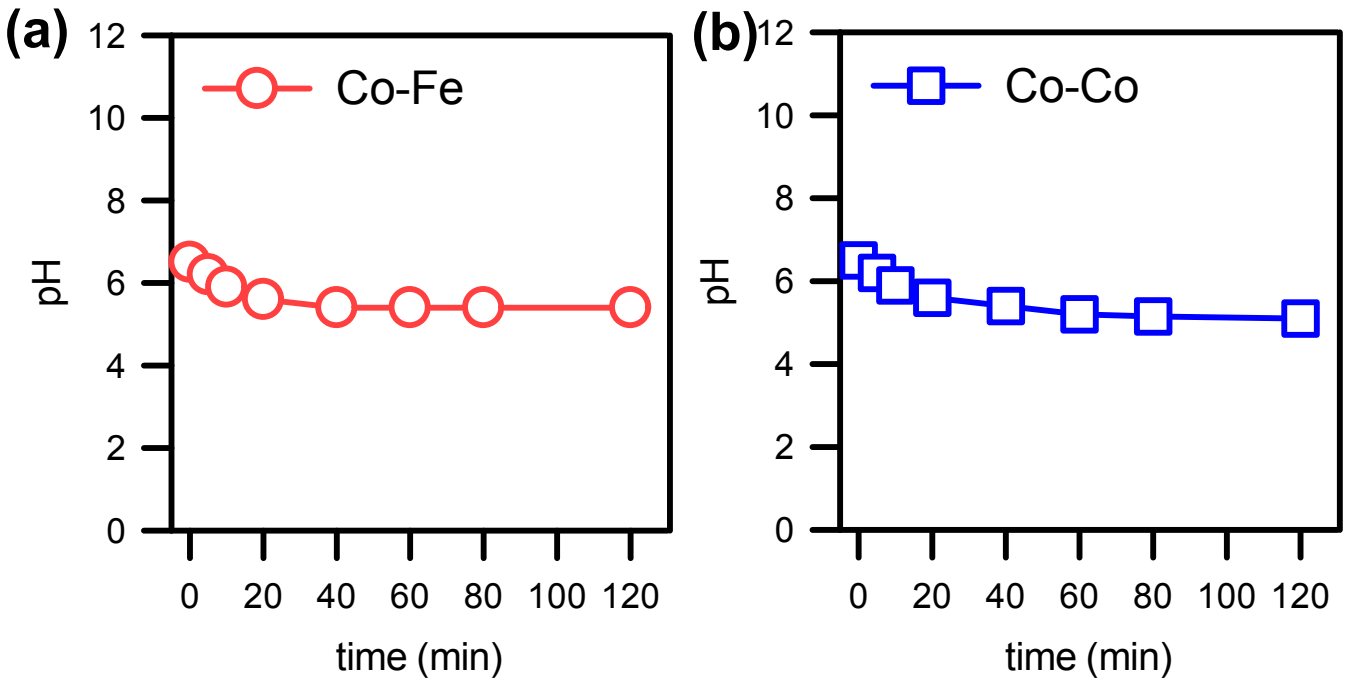

Fig. S7. pH variation during PMS activation by (a) Co-Fe and (b) Co-Co

(PBA = 50 mg L^{-1}; RhB = 10 mg L^{-1}; PMS = 50 mg L^{-1}).

.

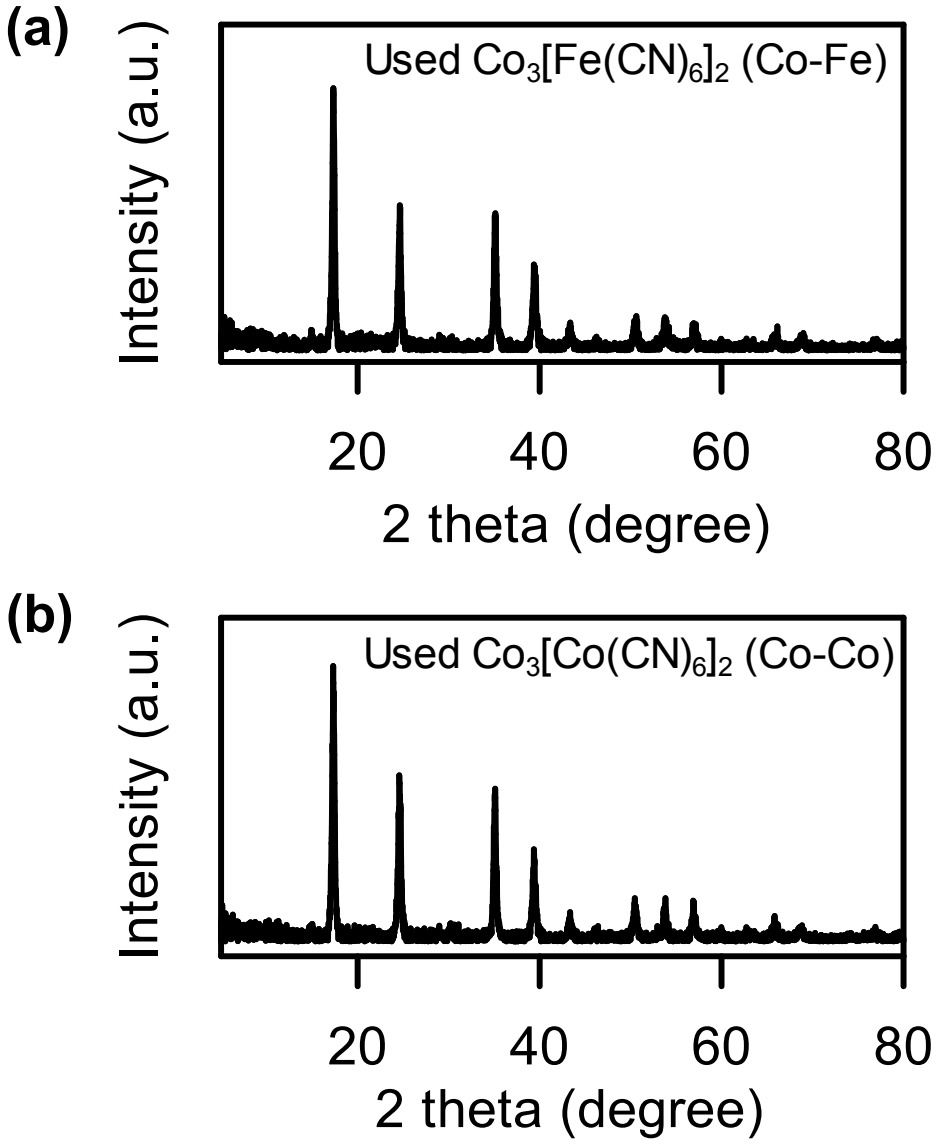

Fig. S8. XRD patterns of (a) used $Co_3[Fe(CN)_6]_2$ and (b) used $Co_3[Co(CN)_6]_2$

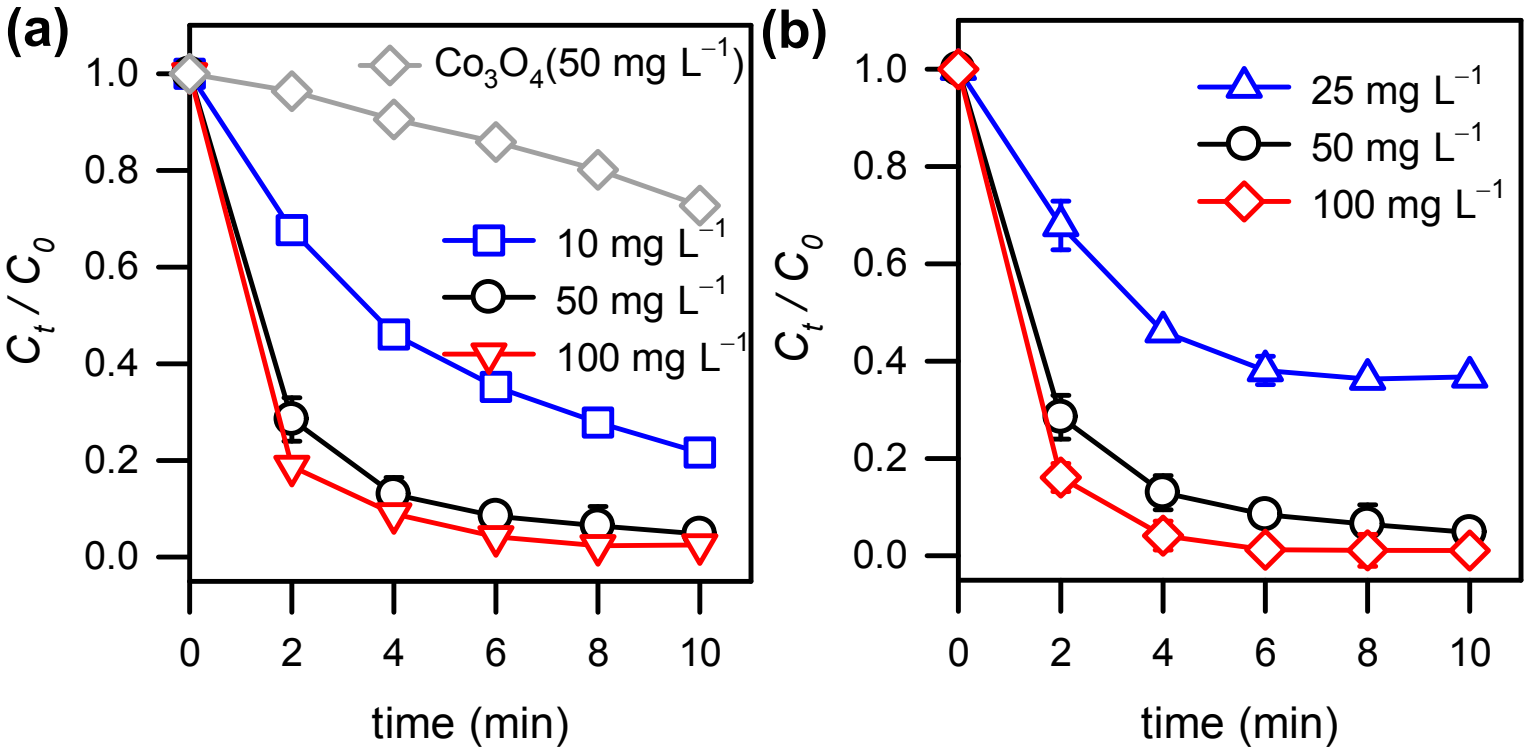

Fig. S9. Effects of (a) Co-Co loading (PMS = 50 mg L^{-1}) and (b) PMS dosage (PBA = 50 mg L^{-1}) on decolorization using $Co[CoCN)_6]_2$ (Co-Co) (RhB = 10 mg L^{-1}; T = 30 °C).

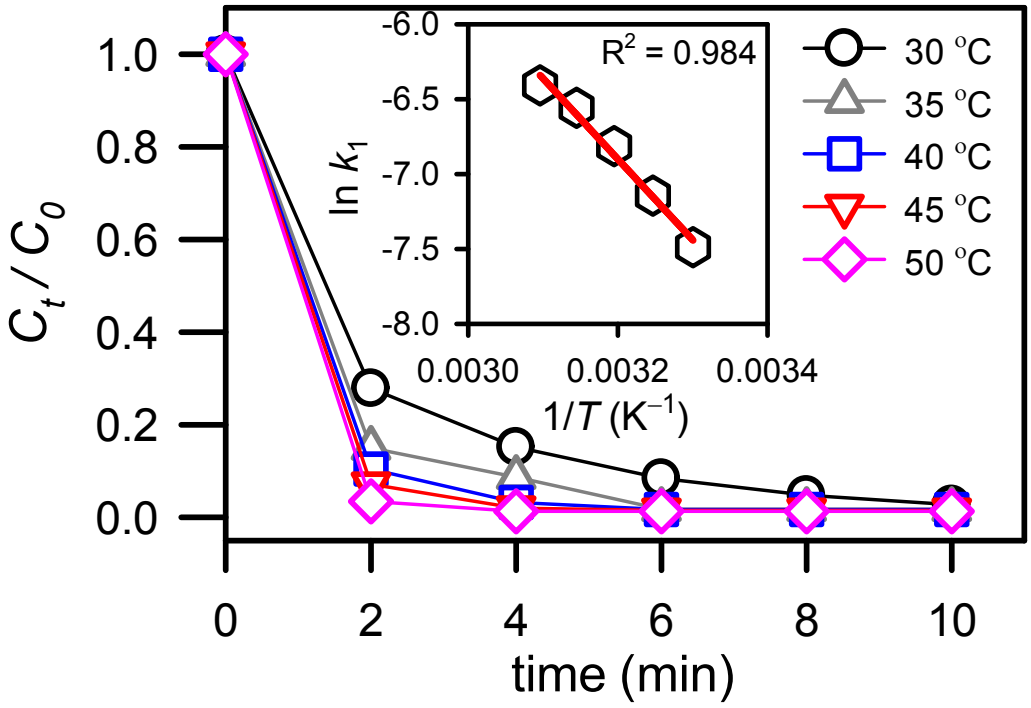

Fig. S10 Effect of temperature on decolorization using Co-Co

(PBA = 50 mg L^{-1}; RhB = 10 mg L^{-1}; PMS = 50 mg L^{-1}).

The inset is a plot for determining the activation energy E_a of RhB

decolorization using PMS activated by Co-Co.

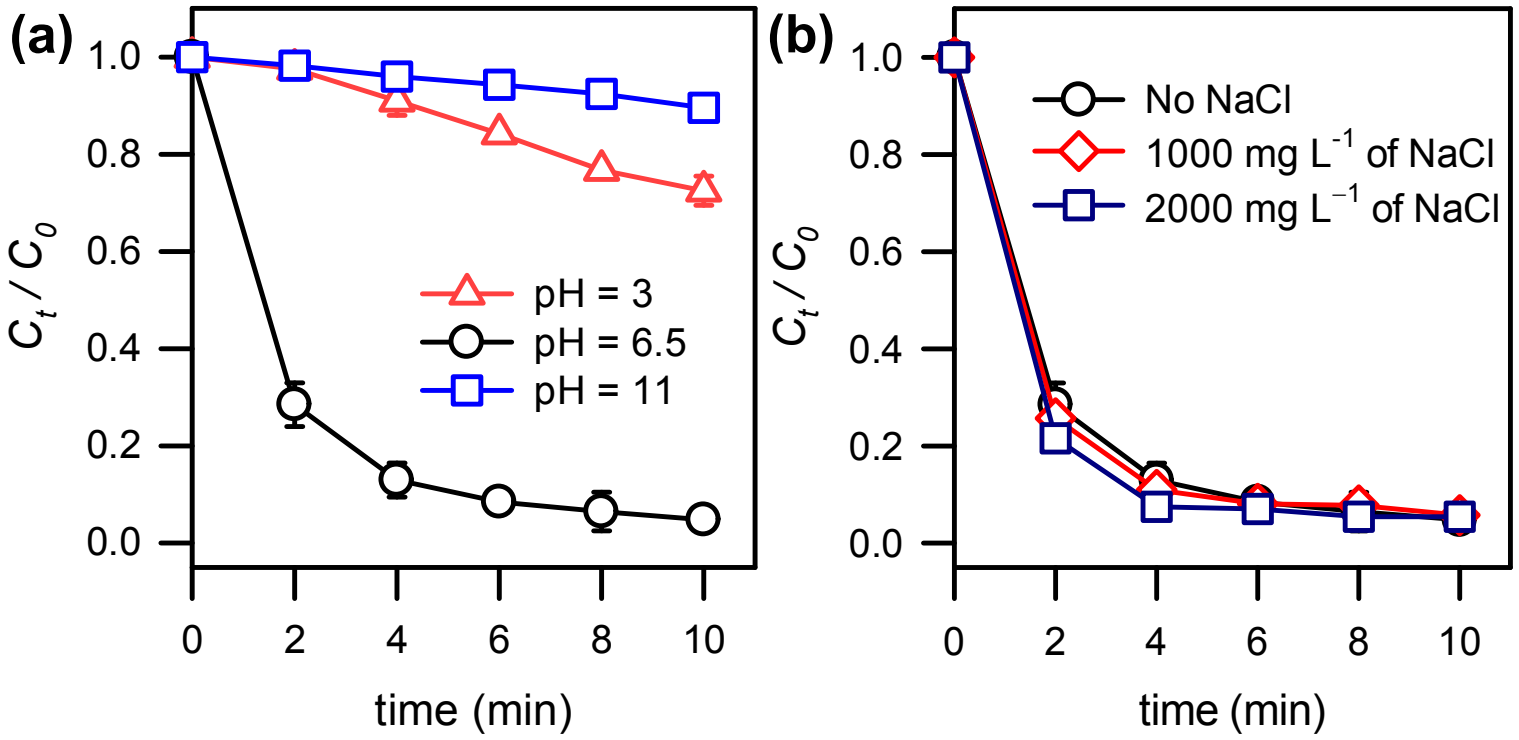

Fig. S11. Effects of (a) pH and (b) salt on decolorization using $Co[Co(CN)_6]_2$ (Co-Co)

(PBA = 50 mg L^{-1}; RhB = 10 mg L^{-1}; PMS = 50 mg L^{-1}; T = 30 °C).

.

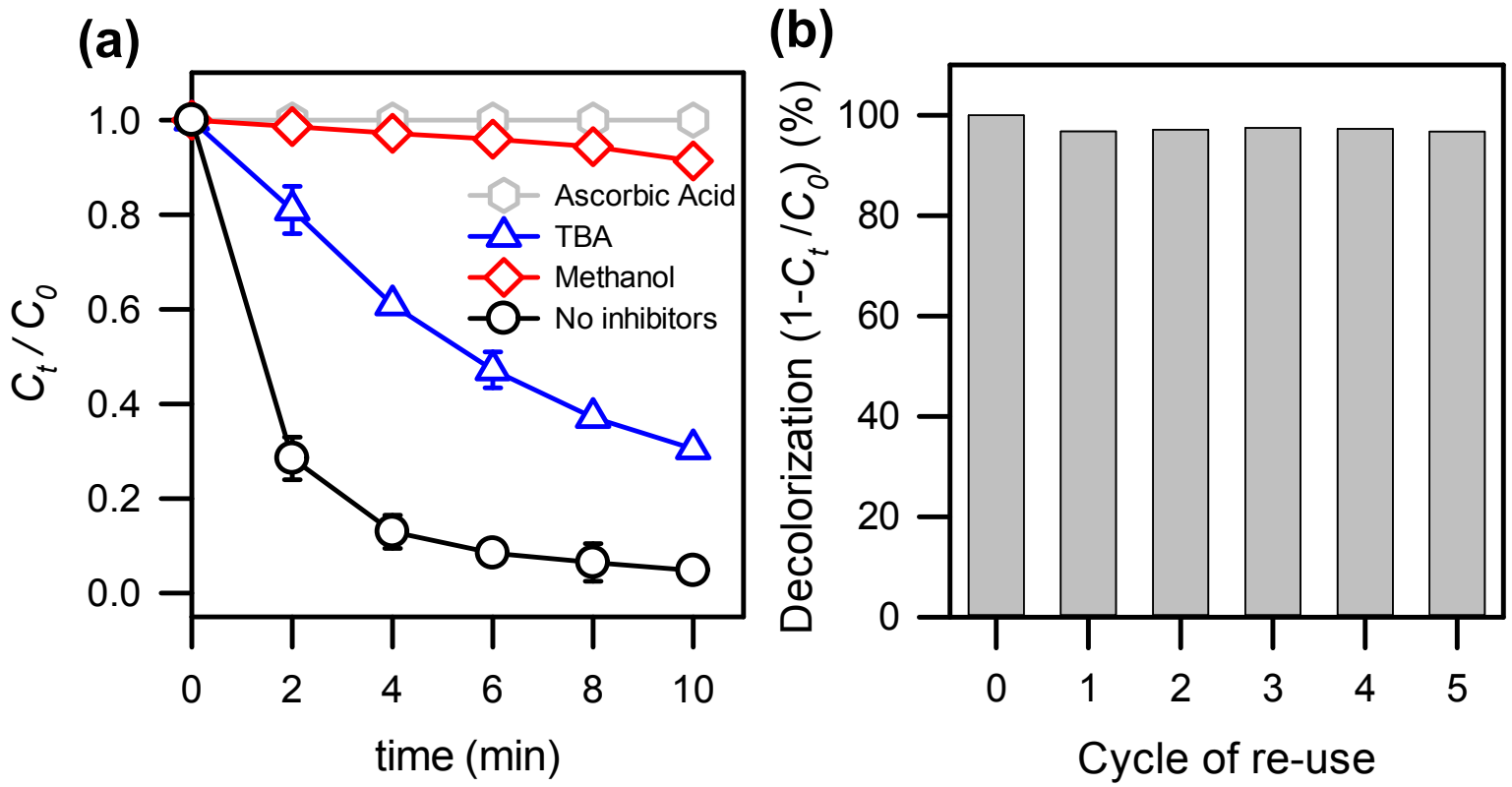

Fig. S12. (a) Effects of inhibitors on decolorization using $Co[Co(CN)_6]_2$ (Co-Co);

(b) recyclability of $Co[Co(CN)_6]_2$ to activate PMS for decolorization

(PBA = 50 mg L^{-1}; RhB = 10 mg L^{-1}; PMS = 50 mg L^{-1}; T = 30 °C).